DOI 10.1007/s11204-023-09866-3
Soil Mechanics and Foundation Engineering, Vol. 60, No. 1, March, 2023 (Russian Original No. 1, January-February, 2023)

EARTHQUAKE-RESISTANT CONSTRUCTION

SEISMIC STABILITY ANALYSIS OF SLOPES USING A PSEUDO-DYNAMIC METHOD COMBINED WITH AN UPPER BOUND METHOD

UDC 624.131.55

Guoxia Shao,[1] Tianze Sun,[2] Ting Li,[3*] and Peng Xu[4]

[1]School of Civil Engineering, Southwest Jiaotong University, Chengdu, China;
[2]School of Science, Changchun University of Science and Technology, Changchun, China;
[3]School of Civil Engineering, Shijiazhuang Tiedao University, Shijiazhuang, China;
[4]State Key Laboratory of Mechanical Behavior and System Safety of Traffic Engineering Structures, Shijiazhuang Tiedao University, Shijiazhuang, China,
*Corresponding author Email: liting9225@126.com.

Pseudo-static methods are commonly employed to analyze slope stability in seismic design, but these methods neglect ground acceleration characteristics (i.e., frequency and duration). In this paper, a pseudo-dynamic method, combined with a kinematic limit analysis method, was developed to calculate the translational seismic stability of slopes with a weak layer, based on the two-part wedge failure mechanism. The proposed method was validated against results from different limit equilibrium methods. Parametric analyses were also conducted to investigate the effects of loading time, frequency, vertical acceleration, slope geometry, and soil strength on slope stabilities.

Introduction

Translational failure is usually the dominant failure-mode for landfills with leachate collection systems or slopes with weak layers. Limit equilibrium methods are commonly employed to evaluate slope stability. Qian et al. [1] developed a two-part wedge method to calculate safety factors with respect to the issue of translational failure analyses of waste masses on clay soil. Qian and Koerner [2] modified this original two-part wedge method to consider the effects of cohesion on slope stabilities and found that safety factors were substantially influenced by the apparent cohesion for cases with a lower friction angle. Eid et al. [3] calculated stability factors for slopes susceptible to a translational failure and concluded that the two-dimensional limit equilibrium method could underestimates slope stabilities. Zhou and Cheng [4] developed a rigorous limit equilibrium method to analyze the stability of three-dimensional slopes.

Since the velocity field associated with an upper bound solution is compatible with the imposed displacements, limit analysis methods are more rigorous than the previous limit equilibrium methods. Assuming a multiple wedge failure mechanism, Donald and Chen [5] compared the safety factors calculated from their proposed method with those from limit equilibrium methods and concluded that the limit analysis method could accurately predict the failure mechanism and safety factors of slopes. Viratjandr and Michalowski [6] analyzed the stability of slopes subjected to water drawdown using the kinematic approach of limit analysis. Huang et al. [7] proposed a rotational-translational failure mechanism for slopes with a weak layer and compared their calculated results with those from limit equilibrium methods. Xu et al. [8] analyzed the effects of backfill strength on rotational stability of reinforced soil walls.

Pseudo-static methods are usually employed to analyze the stability of slopes under seismic loading, such as an earthquake, where the seismic force is assumed to be a static force with a constant value [9]. This method doesn't, however, consider the effects of ground motion frequency and duration [10]. In this paper, a pseudo-dynamic method, combined with a kinematic limit analysis method, is proposed to calculate the translational seismic stability of slopes with a weak layer. The accuracy of the method is demonstrated by comparing the predicted results with those from different limit equilibrium methods. Parametric analyses are also conducted to study the influences of ground acceleration, soil strength, and slope geometry on the stability of slopes.

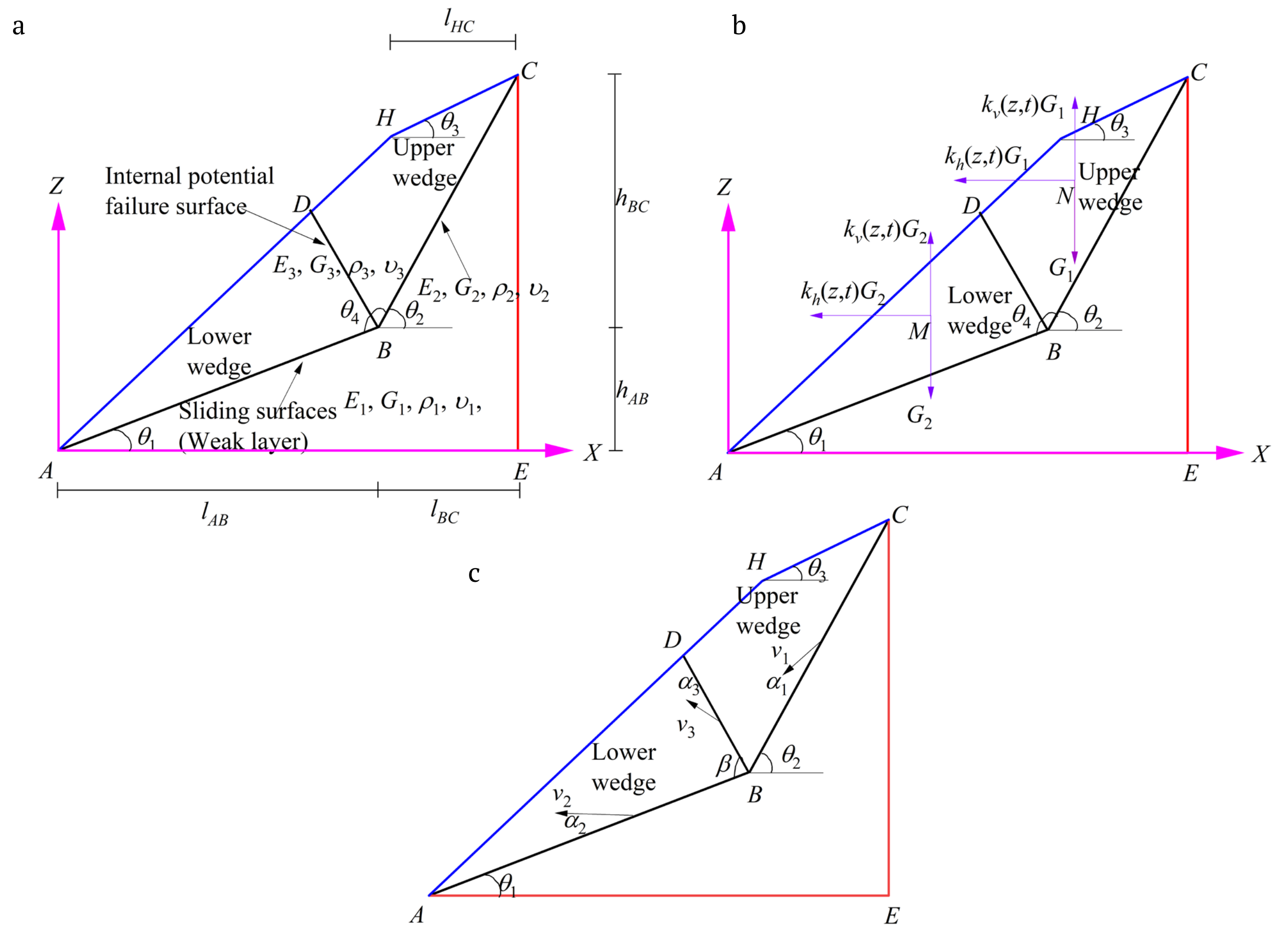

Fig. 1. Sliding failure mechanisms: a) slope models, b) mechanical models, c) kinematically admissible velocity fields.

Methodology

Assumptions

Sliding failures usually occur along with a weak layer within a slope [1] as shown schematically in the cross-sections in Fig. 1. The bilinear line *A-B-C* and the quadrilateral *A-B-C-H* represent a weak layer and a sliding zone, respectively. To implement the method proposed in this paper, the following assumptions are made:

(1) plane strain analysis is employed for the two-dimensional model in Fig. 1,

(2) the failure line *A-B-C* is defined by θ_1 and θ_2, denoting the inclination angles of *AB* and *BC*, respectively, and θ_3 is the inclination angle of *HC*,

(3) a two-part wedge failure mechanism is assumed. The whole sliding zone is divided into an upper and lower wedge by line *BD*, which is an internal potential failure line,

(4) the slope is subjected to harmonic horizontal and vertical base accelerations with amplitudes of k_h and k_v, respectively. The horizontal and vertical seismic coefficients, $k_h(z, t)$ and $k_v(z, t)$ acting at elevation z and time t are expressed as [10]:

$$k_h(z,t) = k_h\left[1 + \frac{\sum_{j=1}^{j=3} z_j}{h}(f_{a-h} - 1)\right]\sin\left[\omega_h\left(t - \sum_{j=1}^{j=3}\frac{z_j}{v_{s-j}}\right)\right], \tag{1a}$$

$$k_v(z,t) = k_v\left[1+\frac{\sum_{j=1}^{j=3} z_j}{h}(f_{a-v}-1)\right]\sin\left[\omega_v\left(t-\sum_{j=1}^{j=3}\frac{z_j}{v_{p-j}}\right)\right], \tag{1b}$$

where $h = h_{AB} + h_{BC}$ is the slope height; f_h and f_v are the horizontal and vertical acceleration amplification factors, respectively; ω_h and ω_v are the horizontal and vertical acceleration angular frequencies, respectively, $\omega_h = 2\pi/T_h$ and $\omega_v = 2\pi/T_v$ (T_h and T_v are the horizontal and the vertical acceleration periods); z_j (j = 1, 2, 3) is the propagation distance in zone *AECB*, the weak layer, and the sliding zone, respectively; and v_{p-j} and v_{s-j} (j = 1, 2, 3) are the primary and shear wave velocities in zone *AECB*, the weak layer, and the sliding zone, respectively, which can be expressed as:

$$v_{s-j} = \sqrt{\frac{G_j}{\rho_j}} = \sqrt{\frac{E_j}{2\rho_j(1+\upsilon_i)}}, \tag{2}$$

$$v_{p-j} = \sqrt{\frac{2G_j(1-\upsilon_j)}{\rho_j(1-2\upsilon_j)}}, \tag{3}$$

where υ_j, ρ_j, E_j, and G_j (j =1, 2, 3) are the Poisson's ratio, density, elastic modulus, and shear modulus, respectively.

Since sliding failures are usually caused by the positive horizontal coefficients as shown in Fig. 1b, k_h (z, t) in Eq. (1) cannot be a negative value. Thus, only a half-cycle of Eq. (1) is considered.

The safety factor F is defined as:

$$\left.\begin{aligned} c_{j-m} &= \frac{c_j}{F} \\ \tan\varphi_{j-m} &= \frac{\tan\varphi_j}{F} \end{aligned}\right\}, \tag{4}$$

where c_j and φ_j (j =1, 2, 3) are the drained cohesion and friction angle along failure lines *AB*, *BC*, and *BD*, respectively; and c_{j-m} and φ_{j-m} (j =1, 2, 3) are the reduced drained cohesion and friction angle required to maintain an energy balance for an admissible mechanism along failure lines, respectively.

Analysis

According to the kinematic upper bound theorem of limit analysis, a geotechnical structure will collapse if the rate of external work, W_E, from external loads and body forces exceeds the energy dissipation rate, D_I, of soil along failure lines for any kinematically admissible failure mechanism [8]. This can be expressed as:

$$W_E \le D_I. \tag{5}$$

The admissible sliding mechanism assumed in this study is shown in Fig. 1c, where the lower wedge and the upper wedge move as a rigid body. The velocities v_1, v_2, and v_3 are inclined to the failure lines at angles α_1, α_2, and α_3, respectively. In addition, according to the associated flow rule, α_1, α_2, and α_3 are also the friction angles along failure lines *AB*, *BC*, and *BD*, respectively.

The magnitudes of the velocities v_2 and v_3 can be expressed as a function of v_1 as:

$$v_3 = \frac{v_1\sin(\theta_2-\theta_1+\alpha_2-\alpha_1)}{\sin(\beta-\alpha_2-\alpha_3)}, \tag{6a}$$

$$v_2 = \frac{v_1\sin(\pi+\theta_1-\beta-\theta_2+\alpha_1+\alpha_3)}{\sin(\beta-\alpha_2-\alpha_3)}. \tag{6b}$$

The external work rate, W_E, can be expressed as:

$$W_E = W_{u-i} + W_{u-g} + W_{l-i} + W_{l-g}, \tag{7}$$

where W_{u-i} and W_{u-g} are the external work rates of the upper wedge induced by ground accelerations and its weight, respectively; and W_{l-i} and W_{l-g} are the external work rates of the lower wedge induced by ground accelerations and its weight, respectively.

The external work rates W_{l-g} and W_{l-i} can be calculated as follows:

$$W_{l-g} = S_2 \gamma v_2 \sin(\theta_1 - \alpha_2) = G_2 v_2 \sin(\theta_1 - \alpha_2), \tag{8}$$

$$W_{l-i} = k_{l-h}(z_M, t) G_2 v_2 \cos(\theta_1 - \alpha_2) - k_{l-v}(z_M, t) G_2 v_2 \sin(\theta_1 - \alpha_2), \tag{9}$$

where γ is the unit weight of the sliding body; S_2 is the area of the lower wedge; and $k_{l-h}(z_M, t)$ and $k_{l-v}(z_M, t)$ are the horizontal and vertical coefficients acting at the centroid of the lower wedge, M, respectively.

Similarly, for the upper wedge, W_{u-i} and W_{u-g} can be calculated with:

$$W_{u-g} = \gamma S_1 v_1 \sin(\theta_2 - \alpha_1) = G_1 v_1 \sin(\theta_2 - \alpha_1), \tag{10}$$

$$W_{u-i} = k_{u-h}(z_N, t) G_1 v_1 \cos(\theta_2 - \alpha_1) - k_{u-v}(z_N, t) G_1 v_1 \sin(\theta_2 - \alpha_1), \tag{11}$$

where S_1 is the area of the upper wedge; $k_{u-h}(z_N, t)$ and $k_{u-v}(z_N, t)$ are the horizontal and vertical coefficients acting at the centroid of the upper wedge, N, respectively.

The centroidal coordinates of the upper and lower wedges in a rectangular coordinate system can be determined as follows:

$$z_M = \frac{z_B + z_D}{3}, \tag{12}$$

$$z_N = \frac{z_B + z_D + z_C}{3}, \tag{13}$$

where z_B, z_C, z_D, z_M, and z_N are z-axis coordinates of points B, C, D, M, and N, respectively. Once z_M and z_N are determined, the horizontal and vertical seismic coefficients acting at the centroids of the upper and lower wedges can be obtained with Eqs. (1a) and (1b), respectively.

The energy dissipation rate, D_I, for the slope model in Fig. 1 is expressed as

$$P_i = \sum_{j=1}^{3} \frac{c_j}{F} v_j l_j \cos\alpha_j, \tag{14}$$

where l_j is the length of the failure planes.

Substituting Eqs. (7) and (14) into Eq. (5), the safety factor F at time t, can be calculated:

$$F = F(\beta, t). \tag{15}$$

The minimum safety factor is defined as $F_{\min}$ under the conditions of $0 \leqslant \beta \leqslant \theta_4$ and $0 \leqslant t \leqslant T/2$.

Validation of the Proposed Method

When $k_h(z, t)$ and $k_v(z, t)$ equal k_h and k_v in Eqs. (1a) and (1b), the method developed here reduces to a pseudo-static method. Assuming a two-wedge mechanism, Qian et al. [1] proposed a limit equilibrium method to analyze the translational stability of landfills. In this section, a comparison was made for the case of a landfill with $k_h = 0.3$, $k_v = 0$, $\gamma = 10.2$ kN/m^3, $\theta_1 = 1.1°$, $\theta_2 = 18.4°$, $\theta_3 = 0°$, $\alpha_1 = \alpha_2 = 17°$, $\alpha_3 = 33°$, $h_{BC} = 30$ m, and $l_{HC} = 20$ m. Values of minimum safety factors, $F_{\min}$ from the above two methods and Morgenstern and Price method are shown in Fig. 2.

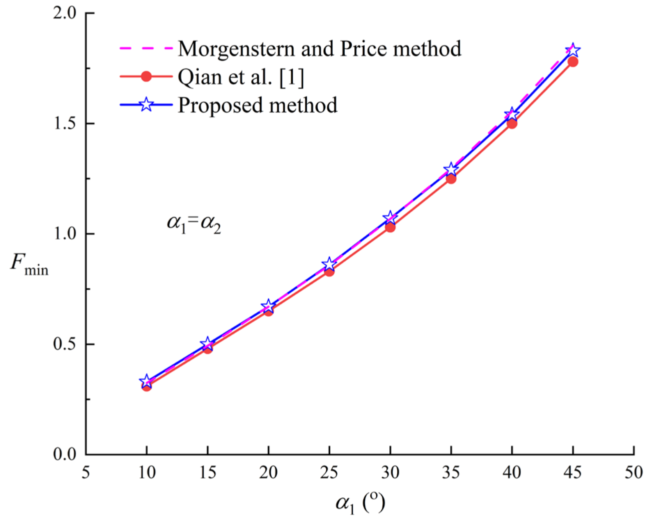

Fig. 2. Predicted F_{min} using different methods.

As shown in Fig. 2, F_{min} values calculated from these three methods all increase with α_1, and the results from the proposed method lie between the results from Morgenstern and Price method and Qian et al. [1]. This proposed method is thus in good agreement with existing methods.

Parametric Analysis

In this section, parametric analyses are performed to investigate the influences of ground acceleration, slope geometry, and soil strength on the safety factors at time t, F, and the minimum safety factors during periods, F_{min}, with the following control values: $\theta_1 = 18^o$, $\theta_2 = 42^o$, $\theta_3 = 0^o$, $l_{AB} = 9$ m, $l_{BC} = 6$ m, $l_{HC} = 1$ m, $k_h = 0.3$, $k_v = 0$, $f_a = 1.3$, $\rho = 22$ kg/m^3, $c_1 = c_2 = 8$ kPa, $\varphi_1 = \varphi_2 = 25°$, $\varphi_3 = 40°$, $v_{s\text{-}1} = 301$ m/s, $v_{s\text{-}2} = 30$ m/s, $v_{s\text{-}3} = 95$ m/s, $v_{p\text{-}1} = 564$ m/s, $v_{p\text{-}2} = 77$ m/s, $v_{p\text{-}3} = 167$ m/s, and $T = T_h = T_v = 1$s.

Ground acceleration

Figure 3a shows the predicted values of F as a function of t for various values of f_a, T, and k_h, calculated using the proposed method and Morgenstern and Price method. The values of F predicted from the pseudo-static method are independent of time. In contrast, since the seismic coefficients are functions of time, F values calculated from the proposed method initially decrease to a minimum value but then increase with t. Furthermore, when the period, T, increases from 1 s to 2 s, the shape of the curve of predicted F changes, but the minimum value of F stays constant. Although the values of F from the proposed method are different depending on the input variables, the minimum value for all cases was obtained at $t = T/4$.Results in Fig. 3a also indicate that the influence of k_h on F is more significant than that of f_a.

Figure 3b shows the minimum safety factor, F_{min}, as a function of k_h for different values of k_v. Similar to the results in Fig. 3a, the predicted values of F_{min} from the proposed method decrease nonlinearly with k_h. The values of F_{min} increase with k_v when k_h is smaller than 0.3. However, a larger vertical ground acceleration coefficient, k_v could decrease the stability of slopes when k_h is greater than 0.3. In addition, the results also indicate that the influence of k_v on F_{min} is more significant when k_h is smaller.

Failure line geometry

To describe the geometry of the sliding line A-B-C in Fig. 4, parameters λ and κ are defined as:

$$\left.\begin{aligned}\lambda &= l_{AB} / (l_{AB} + l_{BC}) \\ \kappa &= h_{AB} / (h_{AB} + h_{BC})\end{aligned}\right\}. \tag{16}$$

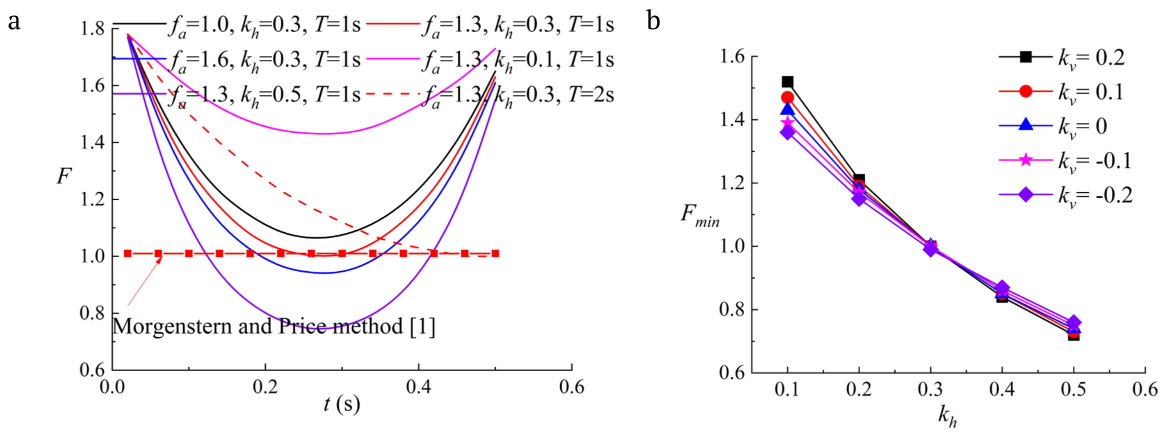

Fig. 3. Predicted F and $F_{\min}$: a) variation of F with f_a, k_h, and T; b) variation of $F_{\min}$ with k_h.

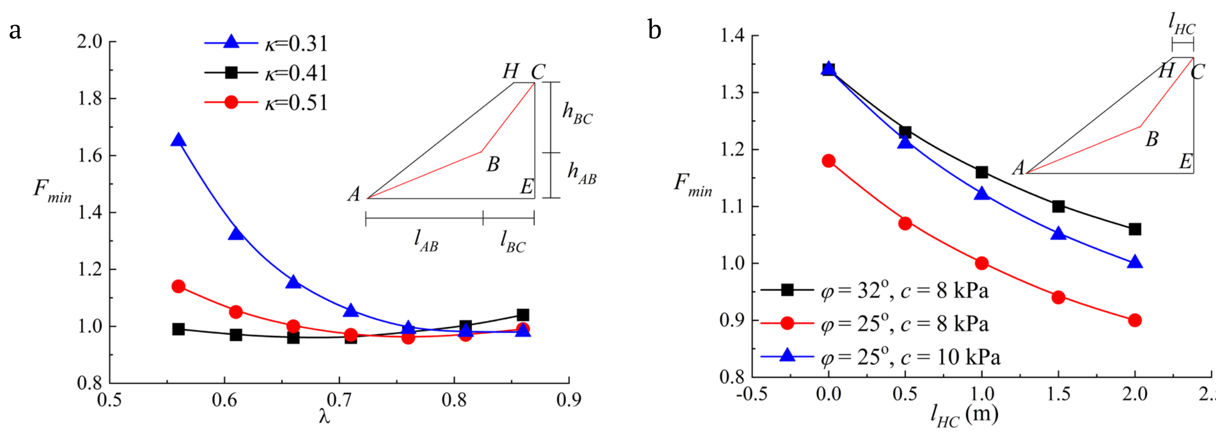

Fig. 4. Variations: a) of F_{min} with λ and b) of F with l_{HC}.

Figure 4a shows variations of $F_{\min}$ with λ given different values of κ. Results show that, overall, F_{min} varies non-uniformly with λ. $F_{\min}$ initially decreases to a minimum value, and then increases with larger λ, particularly for the cases in which $\kappa = 0.31$ and 0.41. This can be attributed to the fact that since the area of the siding body *ABCH* increases with λ when κ is constant, the stability decreases with λ. However, the inclination of *AB* decreases with λ, which could increase the stability of the slope. The results in Fig. 4 also indicate that the influence of λ on F_{min} is more significant when κ is smaller.

Figure 4b shows the influence of the top length of the sliding body, l_{HC}, on $F_{\min}$ with different values of failure surface strength. Results show that $F_{\min}$ decreases non-linearly with l_{HC}, particularly if the failure surface strength is small. Additionally, the predicted values of $F_{\min}$ from the proposed method increase with c and φ. Results in Fig. 5 also show that increasing φ is more effective to increase slope stability, especially if l_{HC} is larger.

Conclusions

A pseudo-dynamic method, combined with a kinematic limit analysis method, has been proposed for the analysis of the translational seismic stability of slopes. The safety factors predicted from the proposed method are in good agreement with results from the Morgenstern and Price method and two-part wedge method. The following conclusions regarding the proposed method are drawn from this study:

1. Safety factors, F, predicted from the proposed method are not constant values but vary with time. The influence of horizontal acceleration coefficient magnitude on F is more significant as compared with the vertical acceleration amplification.

2. If the magnitude of the horizontal base acceleration coefficient magnitude, k_h, is less than 0.3, the minimum safety factor of slopes, $F_{\min}$, increases with the vertical base acceleration coefficient magnitude, k_v. However, a larger vertical acceleration coefficient may reduce the slope stability if k_h is greater than 0.3.

3. Values of $F_{\min}$ calculated from the proposed method increase substantially if the potential failure surface is close to the sliding body surface.

Acknowledgments

This study is funded by Science and Technology Project of Hebei Education Department (No. ZD2021096, QN2021127).

References

1. X. Qian, R. M. Koerner, and D. H. Gray, "Translational failure analysis of landfills," *J. Geotech. Geoenviron. Eng.*, **129**(6), 506-519 (2003).
2. X. Qian and R. M. Koerner, "Effect of apparent cohesion on translational failure analyses of landfills," *J. Geotech. Geoenviron. Eng.*, **130**(1), 71-80 (2004).
3. H. T. Eid, A. M. Elleboudy, H. G. Elmarsafawi, and A. G. Salama, "Stability analysis and charts for slopes susceptible to translational failure," *Can. Geotech. J.*, **43**(12), 1374-1388 (2006).
4. X. P. Zhou and H. Cheng, "Analysis of stability of three-dimensional slopes using the rigorous limit equilibrium method," *Eng. Geol.*, **160**, 21-33 (2013).
5. I. B. Donald and Z. Chen, "Slope stability analysis by the upper bound approach: fundamentals and methods," *Can. Geotech. J.*, **34**(6), 853-862 (1997).
6. C. Viratjandr and R. L. Michalowski, "Limit analysis of submerged slopes subjected to water drawdown," *Can. Geotech. J.*, **43**(8), 802-814 (2006).
7. M. Huang, X. Fan, and H. Wang, "Three-dimensional upper bound stability analysis of slopes with weak interlayer based on rotational-translational mechanisms," *Eng. Geol.*, **223**, 82-91 (2017).
8. P. Xu, K. Hatami, and G. Jiang, "Seismic rotational stability analysis of reinforced soil retaining walls," *Comput. Geotech.*, **118**, 103297 (2020).
9. M. D. Gibson, J. P. Wartman, M. MacLaughlin, and D. K. Keefer, "Pseudo-static failure modes and yield accelerations in rock slopes," *Int. J. Rock Mech. Min. Sci.*, **102**, 1-4 (2018).
10. R. S. Steedman and X. Zeng, "The influence of phase on the calculation of pseudo-static earth pressure on a retaining wall," *Geotechnique*, **40**(1), 103–112 (1990).